# Discovery of Small Molecule CXCR4 Antagonists

Weiqiang Zhan,[†,||] Zhongxing Liang,[‡,||] Aizhi Zhu,[‡] Serdar Kurtkaya,[†] Hyunsuk Shim,*[,‡,§] James P. Snyder,*[,†] and Dennis C. Liotta*[,†]

*Department of Chemistry and Department of Hematology/Oncology, Winship Cancer Institute, and Department of Radiology, Emory University, Atlanta, Georgia 30322*

*Received June 11, 2007*

In light of a proposed molecular mechanism for the C-X-C chemokine receptor type 4 (CXCR4) antagonist **1** (AMD3100), a template with the general structure **2** was designed, and **15** was identified as a lead by means of an affinity binding assay against the ligand-mimicking CXCR4 antagonist **3** (TN14003). Following a structure−activity profile around **15**, the design and synthesis of a series of novel small molecular CXCR4 antagonists led to the discovery of **32** (WZ811). The compound shows subnanomolar potency ($EC_{50}$ = 0.3 nM) in an affinity binding assay. In addition, when subjected to *in vitro* functional evaluation, **32** efficiently inhibits CXCR4/stromal cell-derived factor-1 (SDF-1)-mediated modulation of cyclic adenosine monophophate (cAMP) levels ($EC_{50}$ = 1.2 nM) and SDF-1 induced Matrigel invasion ($EC_{50}$ = 5.2 nM). Molecular field topology analysis (MFTA), a 2D quantitative structure−activity relationship (QSAR) approach based on local molecular properties (Van der Waals radii (VdW), atomic charges, and local lipophilicity), applied to the **32** series suggests structural modifications to improve potency.

## Introduction

The C-X-C chemokine receptor-4 (CXCR4[a]) is a seven-transmembrane G-protein coupled receptor (GPCR) classified as a member of the family I GPCR or rhodopsin-like GPCR family.[1−3] The chemokine stromal cell-derived factor-1 (SDF-1 or CXCL12) is an 8 kDa, 67 residue CXC chemokine peptide, originally isolated from a bone marrow stromal cell line, and it is the natural ligand for CXCR4.[4] The two proteins are rather unique among chemokines and their receptors in that SDF-1 interacts specifically with CXCR4,[5] but more recently SDF-1 was found to bind with an alternative receptor CXCR7.[6] CXCR4 first drew attention as a major coreceptor for the infection of T cell line-tropic (X4) strains of human immunodeficiency virus 1 (HIV-1).[7,8] Interaction between the gp120/CD4 complex and a coreceptor, such as CXCR4 or CCR5, triggers conformational changes in the viral envelope (Env) that lead to membrane fusion and entry of the viral genome into the host cell cytoplasm.[9,10] Importantly, the CXCR4 receptor is expressed much more broadly than chemokine receptors in general, that is, not only on a wide variety of leukocytes but also on cells outside the immune system. Compelling evidence is accumulating that the CXCR4 is far more than a coreceptor for HIV, playing an important role in cancer metastasis, regulation of stem cell trafficking, and neovascularization.[11−14] Consequently, therapeutic strategies to block the interaction between CXCR4 and SDF-1 hold promise for a variety of clinical applications.

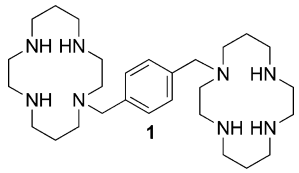


**Figure 1.** Structure of the nonpeptidic CXCR4 antagonist **1**.

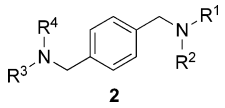


**Figure 2.** Potential CXCR4 antagonist template.

Since the identification of human immunodeficiency virus (HIV) as the causative agent of the acquired immune deficiency syndrome (AIDS) and the disclosure of CXCR4 as a coreceptor for HIV entry, various peptide CXCR4 antagonists, such as T140 and low molecular weight pseudopeptide CXCR4 antagonists, have been reported.[15−19] However, disclosure of nonpeptidic small molecule CXCR4 antagonists has been limited.

Bicyclam-containing small molecular CXCR4 antagonist **1** (AMD3100[7]) was the first CXCR4 antagonist to enter clinical trials for treatment of HIV infection. It was discovered as an anti-HIV agent long before it was understood that it functions by specific blockade of the CXCR4 receptor.[7,16] At physiological pH, the cyclam ring is doubly charged carrying an overall charge of $2^+$ and can adopt a stable *trans*-III *R,R,S,S*-type conformation with respect to the four nitrogen atoms.[17] The protonated cyclam has the propensity to form a direct, hydrogen-bonded complex with a carboxylic acid group in a putative interaction model between **1** and CXCR4.[2,3,17] The latter model suggests that one cyclam ring might be "sandwiched" between Asp262 and Glu318 residues in the receptor, while the disposition of the other ring is compatible with binding to Asp171 at the other end of the main ligand-binding pocket.[2]

* To whom correspondence should be addressed. Dennis C. Liotta, Department of Chemistry, Emory University, 1521 Dickey Drive, Atlanta, Georgia 30322. Telephone: 404-727-6602. Fax: 404-712-8679. E-mail: dliotta@emory.edu. James P. Snyder, Department of Chemistry, Emory University, 1521 Dickey Drive, Atlanta, Georgia 30322. Telephone: 404-727-2415. Fax: 404-712-8679. E-mail: jsnyder@emory.edu. Hyunsuk Shim, Winship Cancer Institute, Emory University, 1365C Clifton Road, N.E., C5008, Atlanta, Georgia 30322. Telephone: 404-778-4564. Fax: 404-778-5550. E-mail: hshim@emory.org.

† Department of Chemistry.

‡ Department of Hematology/Oncology.

§ Department of Radiology.

|| W.Z. and Z.L. contributed equally to this work.

[a] Abbreviations: CXCR4, C-X-C chemokine receptor type 4; SDF-1, stromal-derived factor-1; cAMP, cyclic adenosine monophosphate; AIDS, acquired immune deficiency syndrome; HIV, human immunodeficiency virus; EC, effective concentrations; MFTA, molecular field topology analysis; PLS, Partial Least Squares; QSARs, quantitative structure−activity relationships; TR-FRET, time resolved-fluorescence resonance energy transfer; TLC, thin layer chromatography; H&E, hematoxylin and eosin.

10.1021/jm070679i CCC: $37.00 © 2007 American Chemical Society
Published on Web 10/24/2007

**Table 1.** Structures and Activity of Selected Compounds for Initial Screening

| Compd. | Structure | EC (nM)[a] | Compd. | Structure | EC(nM)[a] |
|---|---|---|---|---|---|
| **4** | 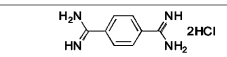 | >1000 | **13** | 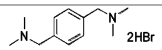 | >1000 |
| **5** | 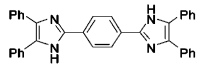 | >1000 | **14** | 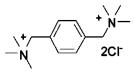 | >1000 |
| **6** | 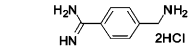 | >1000 | **15** | 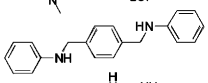 | 10 |
| **7** | 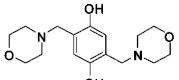 | >1000 | **16** | 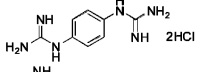 | >1000 |
| **8** | 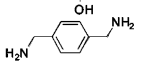 | >1000 | **17** | 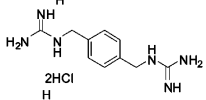 | >1000 |
| **9** | 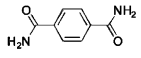 | >1000 | **18** | 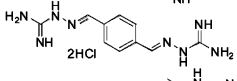 | 100 |
| **10** | 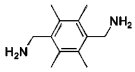 | >1000 | **19** | 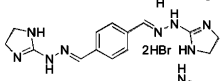 | >1000 |
| **11** | 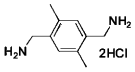 | >1000 | **20** | 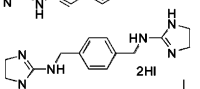 | >1000 |
| **12** | 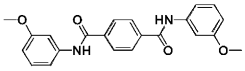 | >1000 | **21** | 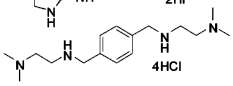 | >1000 |

[a] In this paper, EC (effective concentration) is defined as the concentration at which the compound still elicits a positive response in the peptidic CXCR4 antagonist **3** competition assay.

Mutation of Asp171 and Asp262 to alanines in the CXCR4 chemokine receptor also suggests that the negatively charged aspartate residues at positions 171 and 262, located in transmembrane domains IV and VII, respectively, may represent crucial sites for electrostatic interaction of the positively charged bicyclam rings. The highly basic V3 loop of the gp120 envelope protein of certain HIV-1 strains conceivably operates in a similar fashion.[20]

Although antagonist **1** binds specifically to CXCR4 and is effective as an anti-HIV agent, it was withdrawn from phase II clinical trials in May 2001 due to cardiotoxicity.[21,22] In addition, a specific pharmacokinetic deficit of **1** is its lack of oral bioavailability.[21,23] Another orally bioavailable compound, AMD070, is currently behind the recruitment of patients for a phase I/II trial for HIV patients.[24,25]

In the present study, we designed and synthesized a series of candidate compounds[26] with the general structure **2** based on overlapping structural features with cyclam-containing **1**, presumably resulting in a similar binding mode to the CXCR4 receptor.[2,3,27] The cyclam moieties in **1** (Figure 1) were replaced by *N*-containing basic centers which not only are capable of binding to acidic residues in CXCR4 but also eliminate potential toxicity originating from the possible coordination of the cyclam rings with metal ions (Figure 2).[28−31]

To test the activity of the designed compounds, a competitive binding assay utilizing the potent, peptidic CXCR4 antagonist **3** (TN14003, see the Supporting Information for its structure[13]) was employed. Previously, we reported that peptide **3** blocks the CXCR4 receptor by effectively competing with its ligand SDF-1. The peptidic antagonist **3** also inhibits CXCR4/SDF-1-mediated invasion *in vitro* and obstructs metastasis *in vivo* with high specificity.[13] In addition, two functional assays measuring cyclic adenosine monophosphate (cAMP) production and Matrigel (a basement membrane[32]) invasion were performed to study the selected candidates' roles as antagonists in CXCR4/SDF-1-mediated processes. Furthermore, we developed a quantitative structure−activity relationship (QSAR) based on molecular field topology analysis (MFTA).[33,34]

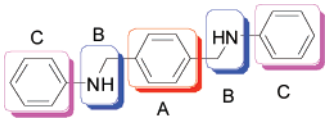


**Figure 3.** The three sectors of **15** subjected to synthetic modification as an approach to potential CXCR4 antagonists.

**Scheme 1**

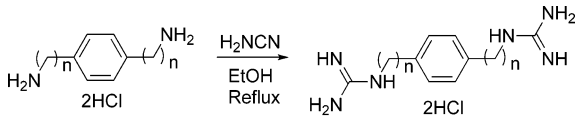


**16**, n=0, 42%
**17**, n=1, 36%

## Results and Discussion

**Initial Screening.** The discovery and development of effective, small molecule peptide mimics remains a major focus for many medicinal chemistry programs. Previously, we and others have shown that T140 analogues, including peptide **3**, bind to the ligand binding site of CXCR4, block the CXCR4/SDF-1 interaction, and intervene in the progression of cancer metastasis.[13,15,35−37] However, because peptides oftentimes exhibit poor druglike properties, we sought to identify a novel series of potent, small molecule antagonists that might prove to be practical for preclinical advancement and progression into clinical evaluation using **3** as the primary screening tool for the binding competition assay. Following our lead design rationale, screening was initiated with various compounds in which two strong basic centers were connected by a phenyl-containing bridge (Table 1). Compounds **4**−**15** are commercially available, and they were subjected to competitive affinity assay without further purification. Guanidine derivatives **16** and **17** were prepared by allowing cyanamide to react with the corresponding ammonium hydrochloride salts (Scheme 1).[38] Hydrazone derivatives **18** and **19** were obtained by condensation of aldehyde and amino guanidines (Scheme 2).[39,40] Dihydroimidazol **20** was prepared by an addition−elimination reaction

**Scheme 2**

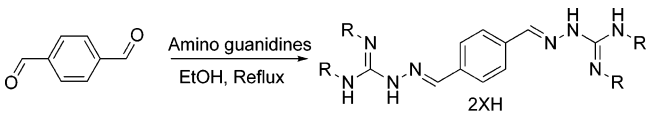


**18**, R=H, X=Cl, 36%
**19**, R= -$CH_2CH_2$-, X=Br, 42%

**Scheme 3**

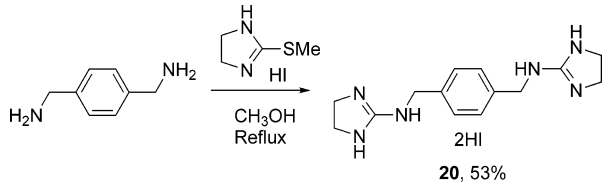


**20**, 53%

**Scheme 4**[a]

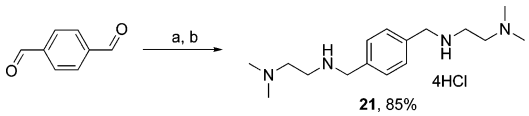


**21**, 85%

[a] Reagents and conditions: (a) *N*,*N*-dimethylethanediamine, $NaBH(OAc)_3$, $ClCH_2CH_2Cl$; (b) HCl/EtOH, $Et_2O$.

involving *p*-xylylenediamine and 2-(methylmercapto)-2-imidazoline (Scheme 3).[40] Amine **21** was synthesized by one-pot reductive amination of an aldehyde and amine in the presence of the reducing reagent $NaBH(OAc)_3$ (Scheme 4).[41]

From the initial screening results, *N*,*N*′-diphenyl-*p*-xylylenediamine **15** and guanylhydrazone **18** were found to be active in the competitive affinity assay with effective concentrations (EC) of approximately 10 and 100 nM, respectively (Table 1). Since amine **15** is more active than **18**, it became our de facto lead around which we further pursued potential CXCR4 antagonists.

**Structure−Activity Relationship (SAR) Study.** Although the initial screening yielded **15** as a lead, the compound was shown to possess a poor pharmacokinetic profile (data not shown). Accordingly, an SAR was developed by manipulation of the three sectors of structure **15** as illustrated in Figure 3, namely, the central aromatic ring A, the intermediate linkers B, and the distal phenyl rings C.

**Sector A: Central Aromatic Ring.** To probe the spatial influence of the flat central phenyl ring, a saturated cyclohexane ring replacement, **24a**, was prepared. Combining the precursor dicarboxylic acid with $SO_2Cl_2$ gave the corresponding acid chloride that was subsequently allowed to react with aniline to provide amide **23**. The latter is easily reduced by $LiAlH_4$ to deliver the target amine **24a** with a central cyclohexane linker (Scheme 5).[42] Surprisingly, **24a** proved to be completely inactive (Table 2), suggesting that a central linker with a planar or near planar geometry is crucial for maintaining activity. To further study the importance of the central aromatic ring on activity, compounds **24b**, **25a** and **25b** were prepared by a reductive amination procedure similar to that used for **21**, while **26a** was synthesized by $S_N2$ displacement (Scheme 6). Compound **25b** was included because many anthracene-containing compounds with at least one basic center have proven to be effective antitumor agents by intercalating to DNA.[39] The competition binding assay indicated no significant difference between **24b**, **25b**, and **26a**, while **25a** proved to be 10-fold more active.

In subsequent experiments, the position and number of anilinomethyl substituents on the central phenyl ring were varied (entries 6−9, Table 2). Compound **27** was obtained from commercial sources, while trisubstituted **29** was prepared by a two-step sequence (Scheme 7). The results show that analogues with one or three $PhNHCH_2$ moieties (**27** and **29**) are unable to block the CXCR4 receptor (Scheme 7). The *meta*-disubstituted analogue **25c** exhibits CXCR4 affinity similar to *para*-disubstituted **15**, while the affinity of *ortho*-disubstituted **26b** decreases by 10-fold.

**Sector B: Amine Linker.** Initial modifications involved the introduction of methyl groups to the linkages between aromatic rings as depicted by **30a** and **30b** (Scheme 8). The methyl groups on the benzylic carbons were expected to exert a conformational bias on the terminal rings relative to **15**, while those on nitrogen were intended to increase the hydrophobicity and basicity of the heteroatom. Both substitutions reduce the affinity to about 50−100 nM (entry 1 and 2, Table 3). Thus, it would appear that an NH group is necessary to retain the high affinity shown by **15**. Second, one or more carbons or nitrogens were inserted between the central and terminal phenyl rings (**24c** and **30c**−**d**, entries 3−5, Table 3). In **24c**, the $CH_2CH_2NH$ moiety caused complete loss of activity even though the extra N is potentially available for binding to the aspartic acid residue in CXCR4. In **30c** and **30d**, the extra carbon also reduced the potency. In summary, modification of sector B illustrates that a terminal phenyl ring connected directly to an unalkylated nitrogen center results in the best activity for the modifications tested.

**Sector C: Terminal Phenyl Rings.** Several electron-withdrawing groups were introduced onto the *para* position of the terminal phenyl rings by combining the dialdehyde with various aniline derivatives (Scheme 9). The CXCR4 competition assay demonstrates that none of the compounds block the chemokine (**31a**−**c**, entries 1−3, Table 4). Conversely, electron-donating substituents at the *para* position retain low EC values as illustrated by the *para*-methoxy in **31d** and alkyl in **31e** and **31f**. By contrast, electron-donating and electron-withdrawing substituents at the *meta* and *ortho* positions elicit mixed effects on activity (**31g**−**l**, entries 7−12, Table 4). For example, **31g** (*m*-F) exhibits an effective concentration of 100 nM, while **31k** (*o*-F), **31h** (*m*-$NO_2$), and **31i** (*m*-OMe) experience a 100-fold improvement by comparison (EC = 1 nM). Surprisingly, **31l** (*o*-OMe) is 10-fold less active, while **31j** (*m*-$CF_3$) is completely unable to block the action of peptide **3** on CXCR4.

As a working hypothesis, we speculated that the poor pharmacokinetic profile of **15** might be the result of rapid oxidative metabolism and that inclusion of a nitrogen atom in terminal aromatic rings might impede this process. The above SAR profile suggested that a 2-pyridyl substituent might be a good initial choice to assess the merits of our hypothesis. This pyridine-containing compound **32** (WZ811) was easily prepared by one-pot reductive amination (Scheme 10) by two-step procedures described previously.[43,44] The competition binding assay indicates that **32** is able to effectively inhibit **3** binding to CXCR4 at an extremely low concentration ($EC_{50}$ = 0.3 nM) (Figure 4). To further evaluate its activity as a potential CXCR4 antagonist, **32** was subjected to two functional assays with encouraging results as discussed below.

**cAMP Assay and Invasion Assay.** We originally planned to subject promising CXCR4 antagonists to the calcium mobilization assay utilized by Hatse et al. to show that **1** is specific against CXCR4.[45] However, a general consensus concerning the GPCR pathway has recently emerged that the heterotrimeric guanosine 5′-triphosphate (GTP) regulatory Gs proteins stimulate cAMP production, while the pertussis toxin-sensitive Gi proteins reduce cAMP.[46,47] We determined an absorption increase at 665 nm by various concentrations of SDF-1 (0−200 ng/mL) to estimate the $EC_{80}$ to be 150 ng/mL

**Scheme 5**[a]

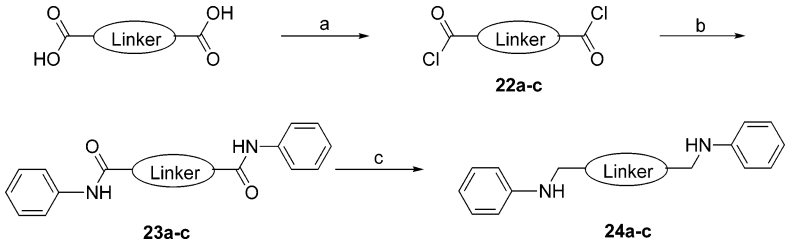


[a] Reagents and conditions: (a) $SO_2Cl_2$, reflux; (b) aniline, pyridine, $CH_2Cl_2$; (c) $LiAlH_4$, THF, reflux.

**Table 2.** CXCR4 Blockade for Analogues with Variations in the Central Ring (Sector A)

| Entry | Compd | Structure | EC(nM) | Entry | Compd | Structure | EC(nM) |
|---|---|---|---|---|---|---|---|
| 1 | **24a** | 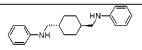 | >1000 | 6 | **25c** | 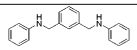 | 10 |
| 2 | **24b** | 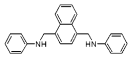 | 100 | 7 | **26b** | 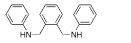 | 100 |
| 3 | **25a** | 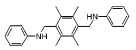 | 10 | 8 | **27** |  | >1000 |
| 4 | **25b** | 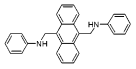 | 100 | 9 | **29** | 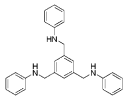 | >1000 |
| 5 | **26a** | 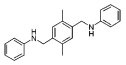 | 200 | | | | |

**Scheme 6**[a]

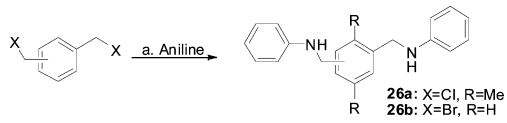


[a] Reagents and conditions: (a) **26a**, pyridine, EtOH, reflux; **26b**, pyridine, EtOH, −20 °C.

**Scheme 7**

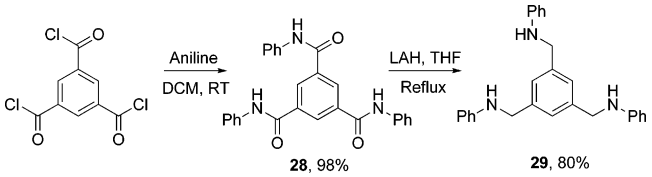


**Scheme 8**

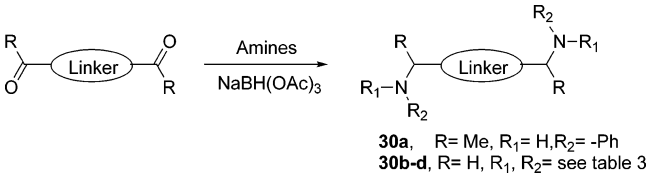


(data not shown). With pretreatment by **32** (15 min at room temperature), the effect of 150 ng/mL of SDF-1 on cAMP reduction is significantly reduced in a dose dependent manner. Compound **32** is effective in counteracting SDF-1 function at doses as low as a few nanomoles, while **1** is only effective at approximately 1000 nM (Figure 5).

We previously reported that peptidic antagonist **3** effectively blocks SDF-1-mediated Matrigel invasion in an assay using SDF-1 as a chemoattractant.[13] Thus, the compounds discussed above with a general structure **2** were examined in the same assay. As shown in Figure 6, **32** is effective at blocking SDF-1 induced invasion. This is consistent with the data displayed in Figure 4 in which **32** is shown to be as potent as **3** in blocking SDF-1-mediated invasion when tested at the same concentration ($EC_{50}$ = 5.2 nM). In addition, cyclam **1** is not as effective as

**Table 3.** CXCR4 Blockade for Analogues with Variations in the Alkylamine (Sector B)

| Entry | Compd | Structure | EC(nM) |
|---|---|---|---|
| 1 | **30a** | 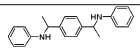 | 50 |
| 2 | **30b** | 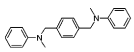 | 200 |
| 3 | **24c** | 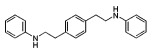 | 100 |
| 4 | **30c** | 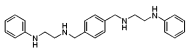 | >1000 |
| 5 | **30d** | 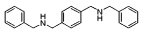 | 80 |

**Table 4.** CXCR4 Blockade for Analogues with Variations in the Terminal Rings (Sector C)

| Entry | compd | *R* | EC (nM) | Entry | compd | R | EC (nM) |
|---|---|---|---|---|---|---|---|
| 1 | **31a** | *p*-CN | 1000 | 7 | **31g** | *m*-F | 100 |
| 2 | **31b** | *p*-$NO_2$ | 1000 | 8 | **31h** | *m*-$NO_2$ | 1 |
| 3 | **31c** | *p*-F | 1000 | 9 | **31i** | *m*-OMe | 1 |
| 4 | **31d** | *p*-OMe | 25 | 10 | **31j** | *m*-$CF_3$ | 1000 |
| 5 | **31e** | *p*-Me | 10 | 11 | **31k** | *o*-F | 1 |
| 6 | **31f** | *p*-Et | 20 | 12 | **31l** | *o*-OMe | 10 |

**Scheme 9**

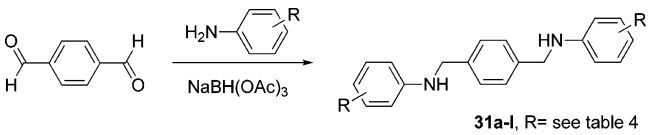


**32** even at a 10-fold higher concentration. Thus, this study demonstrates that **32** is a potent inhibitor of CXCR4-mediated signaling at low nanomolar concentrations.

**Molecular Field Topology Analysis (MFTA) QSAR.** MFTA is an analytical method for generating quantitative structure−activity relationships (QSARs) by topological analysis of a series of closely related compounds associated with a quantitative or semiquantitative biological endpoint.[33,34] The

**Scheme 10**[a]

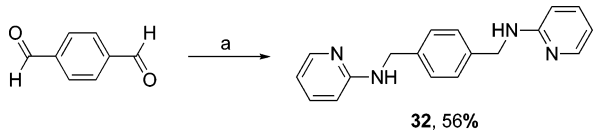


[a] Reagents and conditions: (a) 2-amino-pyridine, $NaBH(OAc)_3$, HOAc, $ClCH_2CH_2Cl$.

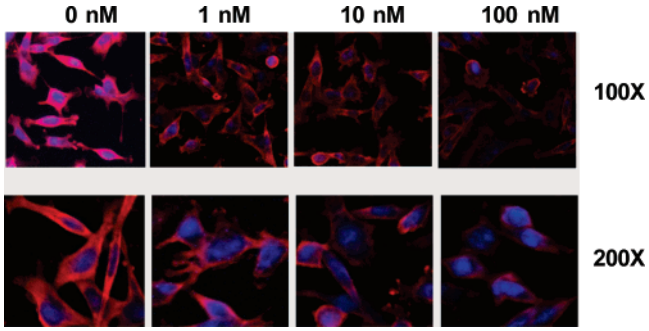


**Figure 4.** Inhibitory efficacy of **32** against peptidic antagonist **3** binding to CXCR4. These results indicate that the $EC_{50}$ is less than 1 nM.

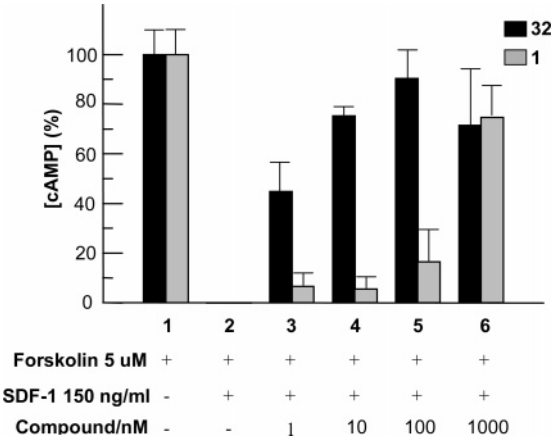


**Figure 5.** Comparison of the inhibition of cAMP production by **32** and **1**. With pretreatment (15 min at room temperature) of **32** or **1** at various concentrations, the effect of 150 ng/mL SDF-1 on cAMP reduction was measured by using the TR-FRET based LANCE assay kit. While **32** is effective in counteracting SDF-1 function at a concentration as low as 10 nM, **1** requires almost 1000 nM to significantly block SDF-1 function. Note that the slight reduction of cAMP% for **32** at 1000 nM is not statistically significant. The effect levels out from 100 to 1000 nM.

approach seeks to model bioactivity in terms of local molecular properties (descriptors). MFTA produces a molecular supergraph for the set of compounds examined, PLS-based (Partial Least Squares) correlation statistics, and a graphical representation of each local descriptor on activity.

In the present application, to supplement the qualitative SAR discussion above, approximate $\log(1/EC_{50})$ values for 16 CXCR4 antagonists (compounds **32**, **12**, **25a**, **26a**, **30a**, **30b**, **31b**−**e**, and **31g**−**l**, Tables 1−4; see the Supporting Information for individual values) were tested against a variety of local descriptor sets. A model was constructed with a predictive $q^2$ value (leave-25%-out cross-validation) of 0.71. The molecular supergraph for **32** is shown in Figure 7 with various compound substituents superimposed on it.

The best results were obtained with a combination of three descriptors:[34] VdW (Van der Waals radii), Q (effective atomic charge; Gasteiger−Marsili), and Lg (local lipophilicity; sum of Ghose−Crippen atomic contributions for an atom and attached hydrogens). The resulting correlation (Figure 8) is characterized

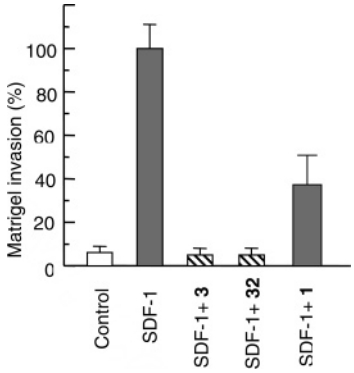


**Figure 6.** Inhibition of CXCR4/SDF-1-mediated invasion of MDA-MB-231 *in vitro* by **32** compared to **3** and **1**. We seeded cells on top of the Matrigel and added SDF-1 to the lower chamber. Invasive cells penetrate the Matrigel and end up on the other side of the Matrigel. We estimated invasion by counting the number of invading cells stained by H&E at the bottom side of the Matrigel chamber and setting the average of the invading cell numbers of MDA-MB-231 with SDF-1 added to the lower chamber as 100%.

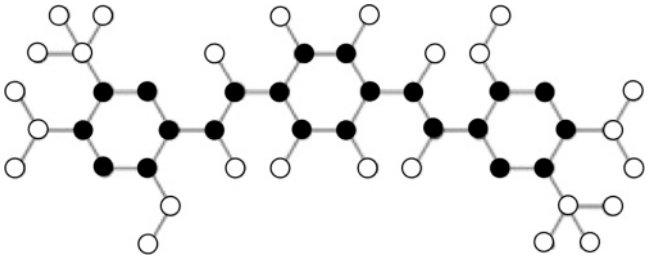

**Figure 7.** MFTA supergraph representing the data set of 16 CXCR4 antagonists with a **32** core (black circles) and various substituents superposed on it (white circles).

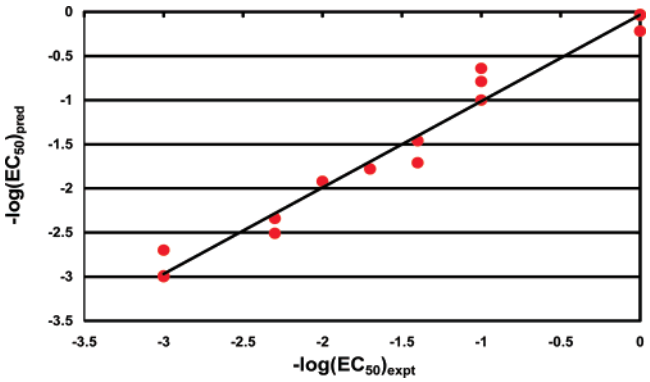


**Figure 8.** MFTA correlation of approximate $EC_{50}$ values for 16 CXCR4 antagonists based on the following descriptors: van der Waals radii (VdW), charge (Q), and lipophilicity (Lg).

by $N = 16$, number of PLS factors $N_F = 8$, $r = 0.99$, $r^2 = 0.98$, and $q^2 = 0.71$ (leave-25%-out cross-validation). Increasing the number of descriptors did not improve the correlation.

The major contributions of the local descriptors to the correlation can be expressed in terms of color-coded supergraphs (Figure 9). At the red-colored positions, an increase in descriptor property implies an *increase* in activity. At the blue-colored positions, an increase suggests a *decrease* in activity.

The VdW supergraph (Figure 9) suggests an activity increase with larger substituents at the red-marked positions. This is reflected in the $EC_{50}$ decrease of 50−100-fold for **31d** and **31e** relative to **31c** by replacing the small *p*-F atom with *p*-OMe and *p*-Me, respectively, in the terminal aromatic rings. A similar activity improvement is observed for **31i** relative to **31g** by

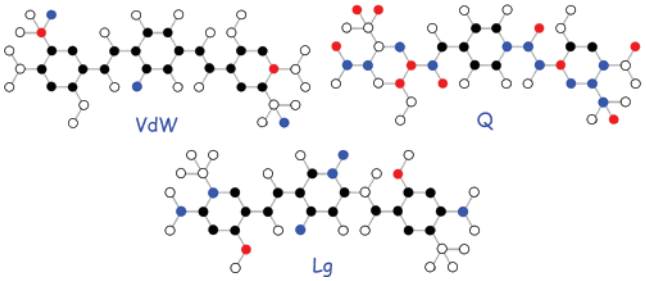


**Figure 9.** Impact on the activity of three local descriptors (VdW, Q, and Lg) expressed on the CXCR4 antagonist supergraph. An increase in the descriptor property at the red and blue positions predicts an increase and a decrease in activity, respectively.

substituting *m*-F by *m*-OMe (Table 4). The central ring space is subject to the same phenomenon as indicated by the slight reduction in $EC_{50}$ for **15** by removal of the four methyl groups in **25a** (Table 2).

The supergraph associated with charge suggests that an increase of charge at the *para* positions of the terminal rings would be beneficial. The 100−1000-fold improvement for **31d** (*p*-OMe) over **31a** (*p*-CN) shows the trend (Table 4). Similarly, the blue centers in this supergraph imply that a reduction of charge should increase activity. The 1000-fold activity gain from *bis*-amide **12** to *bis*-amine **31i** is in agreement. Finally, the operation of the supergraph characterizing changes in lipophilicity (Figure 9) is represented by the replacement of *o*-OMe with the relatively more lipophilic[48−50] *o*-F in **31l** and **31k** (red centers, 10-fold improvement, Table 4) and by the reverse substitution from **31c** (*p*-F, 1000 nM) to **31d** (*p*-OMe, ∼20 nM, blue centers, 50-fold improvement). These observations will be expanded and applied to future syntheses of CXCR4 antagonists.

## Conclusions and Prospects

The current study presents the discovery of a new class of nonpeptide CXCR4 antagonists with low molecular weights and a novel and simple scaffold: two aromatic amine moieties connected by a *para*-xylylene group. The template was designed in part based on structural features embedded in the previously reported CXCR4 antagonist **1**.[2,3,27] It appears to incorporate the critical features necessary for blocking the complexation of CXCR4 by SDF-1 while eliminating the metal-chelating properties of a cyclic polyamine. Screening of the analogues, performed using a competitive affinity binding assay employing the peptidic CXCR4 antagonist **3**, led to the identification of the initial lead **15**. Structure−activity studies around **15** brought to light several important structural insights: (1) the central aromatic ring is critical for high CXCR4 affinity; (2) a one-carbon separation between the central phenyl ring and the nitrogen of the acyclic linker is essential for high potency; (3) anti-CXCR4 activity is much more sensitive to *para* substitution on the terminal aromatic rings compared to *meta* and *ortho* substitution; (4) the SAR profile led to the design and synthesis of **32**, a highly potent competitive blocker of CXCR4 action at sub-nanomolar concentrations; and (5) an MFTA QSAR analysis based on three descriptors suggests additional structural modifications for extending the antagonist class.

Further functional assays demonstrate that **32** can effectively counteract SDF-1 function at low doses and block *in vitro* CXCR4/SDF-1-mediated signaling more effectively than **1**. Future work with **32** will focus on *in vivo* animal model studies and preclinical evaluation. We anticipate that the insights gained from the present study will serve as the basis for the development of novel therapeutic strategies for CXCR4-related diseases. For example, compound **32** has been tested against HIV propagation and it was found to be weakly active in cell culture (Zhan, W.; Liotta, D. et al., unpublished results). Further modification around **32** to increase its anti-HIV activity is in progress.

## Experimental Section

**Initial Screening of Anti-CXCR4 Small Molecules Based on a Binding Affinity Assay.** For compound screening based on a competition binding assay, $2 \times 10^4$ MDA-MB-231 cells in 200 $\mu$L of medium were seeded in an 8-well slide chamber 2 days before the experiments. Various concentrations of different compounds (1, 10, 100, and 1000 nM) were added to the separate wells and incubated for 10 min at room temperature, and then the cells were fixed in 4% ice-cold paraformaldehyde. The cells were rehydrated in phosphate-buffered saline (PBS) and blocked to eliminate nonspecific binding (avidin and biotin blocking solution, Zymed Laboratories, Inc., San Francisco, CA). The slides were subsequently incubated for 45 min at room temperature with 0.05 $\mu$g/mL biotinylated **3**, washed three times with PBS, and incubated in streptavidin-rhodamine (1:150 dilution; Jackson ImmunoResearch Laboratories, West Grove, PA) for 30 min at room temperature. Finally, the slides were washed with PBS and mounted in an antifade mounting solution (Molecular Probes, Eugene, OR), and the samples were analyzed on a Nikon Eclipse E800 microscope.

**Tumor Cell Invasion Assay.** To model *in vitro* metastasis, a Matrigel invasion assay was performed within a Matrigel invasion chamber from BD Biocoat Cellware (San Jose, CA). SDF-1α (200 ng/mL; R & D Systems, Minneapolis, MN) was added to the bottom chamber to induce the invasion of MDA-MB-231 cells through the Matrigel. The selected compounds were added to the cells before the cells were seeded in the top chamber. The Matrigel invasion chamber was incubated for 22 h in a humidified tissue culture incubator. First, noninvading cells were removed from the top of the Matrigel with a cotton tipped swab. Invading cells at the bottom of the Matrigel were fixed in methanol and stained with hematoxylin and eosin (H&E). The invasion rate was determined by counting the H&E stained cells.

**cAMP Assay to Measure $G_i$ Function.** Perkin-Elmer's LANCE cAMP assay kit (catalog #AD0262) based on time-resolved fluorescence resonance energy transfer (TR-FRET) was utilized to determine a compound's ability to block cAMP modulation induced by CXCR4/SDF-1 interaction. Human glioma U87 cells overexpressing CD4 and CXCR4 (U87CD4CXCR4) were seeded at 2500 cells/well in a 384-well plate in 2% FBS 48 h before the test. The experiment was performed according to the manufacturer's instructions using 5 $\mu$M Forskolin to induce cAMP production that is reduced by the presence of SDF-1. Results were measured in a Perkin-Elmer Envision 2102 multilabel reader with the following parameters: flash energy area = low, flash energy level = 239, counting cycle = 1 ms, and ex/em = 340 nm/665 nm.

**Chemistry: General.** Proton and carbon NMR spectra were recorded on INOVA-400 (400 MHz) or INOVA-600 (600 MHz) spectrometers. The spectra obtained were referenced to the residual solvent peak. They were recorded in deuteriochloroform ($CDCl_3$), dimethyl sulfoxide-$d_6$ (DMSO-$d_6$), or deuterium oxide ($D_2O$). Mass spectra were recorded on a JEOL spectrometer at the Emory University Mass Spectrometry Center. Element analyses were performed by Atlantic Mircolab, Inc. (Norcross, GA). Flash column chromatography was performed using Scientific Absorbent Incorporated Silica Gel 60. Analytical thin layer chromatography (TLC) was performed on precoated glass backed plates from Scientific Adsorbents Incorporated (Silica Gel 60 $F_{254}$; 0.25 mm thickness). Plates were visualized using ultraviolet, iodine vapors, or phosphomolybdic acid.

Compounds **1**, **3**−**15**, **27**, **31a**, **31c**−**f**, and **31k** are available from commercial suppliers, and they were tested without further purification.

**General Procedure for Guanidine Hydrochlorides (A). 1,4-Diguanidobenzene Dihydrochloride (16).** The preparation was

performed according to a modified literature procedure.[38] *p*-Phenylenediamine dihydrochloride (1.81 g, 1.0 mmol) and cyanamide (1.26 g, 3.0 mmol) in absolute ethanol (50 mL) were heated under reflux overnight. After condensation, the resulting dihydrochloride was filtered off, washed with diethyl ether, and dried to give a crude product which was recrystallized from hot methanol to give **16** as white crystals (0.81 g, 42% yield). $^1$H NMR (600 MHz, $D_2O$) $\delta$ 7.40 (4H, s); $^{13}$C NMR (150 MHz, $D_2O$) $\delta$ 159.02, 136.36, 129.98. mp 302−304 °C (dec). Anal. Calcd for $C_8H_{12}N_6\cdot$2HCl: C, 36.24; H, 5.32; N, 31.70; Cl, 26.74. Found: C, 36.34; H, 5.34; N, 31.76; Cl, 26.70.

**1,1′-(1,4-Phenylenebis(methylene))diguanidine Dihydrochloride (17).**[51] The title compound was prepared according to general procedure A as a pale white solid in 36% yield. $^1$H NMR (400 MHz, DMSO-$d_6$) $\delta$ 8.08 (2H, s), 7.32 (4H, s), 6.85−7.71 (8H, br), 4.37 (4H, s); $^{13}$C NMR (100 MHz, DMSO-$d_6$) $\delta$ 157.12, 136.61, 127.53, 43.65. mp 278−311 °C (dec). Anal. Calcd for $C_8H_{12}N_6\cdot$2HCl: C, 40.96; H, 6.19; N, 31.66. Found: C, 40.99; H, 6.23; N, 31.31.

**General Procedure for Hydrazone Derivatives (B). 1,4-Bis-[2-(diaminomethylene)carbohydrazonoyl]benzene Dihydrochloride (18).**[52] Terephthaldicarboxaldehyde (0.67 g, 5.0 mmol) and aminoguanidine hydrochloride (1.22 g, 11.0 mmol) in ethanol (25 mL) with ethanolic HCl (2.0 mL) were heated to reflux for 2 h. After cooling to room temperature, the white precipitate was filtered off to give **18** as a pale white solid (1.51 g, 95%). $^1$H NMR (400 MHz, DMSO-$d_6$) $\delta$ 12.31 (2H, s), 8.21 (2H, s), 7.94 (4H, s), 7.60−8.20 (8H, br); $^{13}$C NMR (100 MHz, DMSO-$d_6$) $\delta$ 155.52, 145.98, 135.18, 127.84. mp 316−318 °C (dec). Anal. Calcd for $C_{10}H_{14}N_8\cdot$2HCl$\cdot$0.7$H_2O$: C, 36.20; H, 5.29; N, 33.77; Cl, 21.37. Found: C, 36.07; H, 5.23; N, 33.42; Cl, 21.11.

**1,4-Bis((*E*)-(2-(4,5-dihydro-1*H*-imidazol-2-yl)hydrazono)methyl)-benzene Dihydrobromide (19).**[39] The title compound was prepared according to general procedure B as a pale white solid in quantitative yield. $^1$H NMR (400 MHz, DMSO-$d_6$) $\delta$ 12.39 (2H, s), 8.30−9.20 (4H, br), 8.22 (2H, s), 7.92 (4H, s), 3.75 (8H, s); $^{13}$C NMR (100 MHz, DMSO-$d_6$) $\delta$ 157.80, 147.20, 135.16, 127.81, 42.74. mp 349−352 °C (dec). Anal. Calcd for $C_{14}H_{18}N_8\cdot$2HBr: C, 40.96; H, 6.19; N, 31.66. Found: C, 41.19; H, 6.35; N, 31.31.

***N,N′*-Bis(4,5-dihydro-1*H*-imidazol-2-yl)-1,4-benzenedimethanamine Dihydroiodide (20).**[40] The title compound was prepared according to a modified literature procedure.[39] *p*-Phenylenediamine (544.8 mg, 4.0 mmol) and 2-methylmercapto-4,5-dihydroimidazole hydroiodide (2.06 g, 8.4 mmol) were dissolved in methanol (25 mL). After refluxing overnight, the solution was reduced to minimal volume under reduced pressure, and diethyl either was added, producing a white precipitate. The precipitate was collected and recrystallized in hot methanol to give **20** as a pale white solid (1.12 g, 53%). $^1$H NMR (400 MHz, DMSO-$d_6$) $\delta$ 8.66 (2H, s), 7.60−8.60 (4H, br), 7.31 (4H, s), 4.36 (4H, d, $J$ = 6.0 Hz), 3.60 (8H, s); $^{13}$C NMR (100 MHz, DMSO-$d_6$) $\delta$ 159.31, 136.50, 127.53, 45.06, 42.54. mp 294−296 °C (dec). Anal. Calcd for $C_{14}H_{20}N_6\cdot$2HI: C, 31.84; H, 4.20; N, 15.91. Found: C, 32.06; H, 4.35; N, 15.77.

**General Procedure for the Reductive Amination Product (C). *N,N′*-Bis[2-(dimethylamino)ethyl]-1,4-benzenedimethanamine Tetrahydrochloride (21).**[53] This procedure was performed according to a modified literature procedure.[41] A mixture of terephthaldicarboxaldehyde (0.67 g, 5.0 mmol) and *N*,*N*-dimethyl-1,2-ethanediamine (0.93 g, 1.21 mL, 10.5 mmol) were treated with sodium triacetoxyborohydride (3.18 g, 15.0 mmol) in 1,2-dichloethane (20 mL). After stirring at room temperature under an argon or nitrogen atmosphere until the disappearance of the reactants from the TLC plates, the reaction mixture was quenched by adding aqueous NaOH (1.0 N) and then extracted with diethyl ether (2 × 30 mL). The combined organic phases were washed with brine and dried over anhydrous $MgSO_4$. The solvent was evaporated to give the crude product which could be purified by column chromatography. In this case, the yellow crude residue was dissolved in ethanol, followed by addition of ethanolic HCl dropwise to form a white precipitate which was filtered off, dried, and recrystallized from hot water and ethanol to give **21** as a pale white solid (1.96 g, 85%). $^1$H NMR (600 MHz, $D_2O$) $\delta$ 7.58 (4H, s), 4.37 (4H, s), 3.58 (8H, s), 2.98 (12H, s); $^{13}$C NMR (100 MHz, $D_2O$) $\delta$ 131.95, 130.81, 52.45, 51.30, 43.45, 41.45. mp 250−252 °C (dec). Anal. Calcd for $C_{16}H_{30}N_4\cdot$4HCl$\cdot$2$H_2O$: C, 41.75; H, 8.32; N, 12.17. Found: C, 41.83; H, 8.26; N, 11.92.

**General Procedure for Amines from Reducing Amides (D). *N,N′*-Diphenyl-*trans*-1,4-cyclohexanedimethanamine (24a).** This compound was prepared in two steps starting from commercially available *trans*-1,4-cyclohexanedicarboxylic acid.

**Step 1.** A mixture of *trans*-1,4-cyclohexanedicarboxylic acid (0.69 g, 4.0 mmol) in thionyl chloride (15 mL) was refluxed for 2 h in an anhydrous system with a condenser equipped with a NaOH trap at the top. After removing the excess thionyl chloride under reduced pressure, dichloromethane (50 mL) was added into the resulting carboxylic chloride residue **22a**, followed by the addition of amine (0.73 mL, 8.0 mmol) and pyridine (0.97 mL, 12.0 mmol). The mixture was stirred at room temperature for 1 h. The solvent was reduced to minimal volume under reduced pressure. The white precipitate was filtered off, washed with dichloromethane and water to give crude amide **23a** as a white solid in quantitative yield which was pure enough to use in the next step. $^1$H NMR (600 MHz, DMSO-$d_6$) $\delta$ 9.86 (2H, s), 7.61 (4H, d, $J$ = 7.8 Hz), 7.31 (4H, t, $J$ = 7.8 Hz), 7.02 (2H, d, $J$ = 7.8 Hz), 2.35 (2H, br), 1.91 (4H, d, $J$ = 7.2 Hz), 1.49 (4H, m); $^{13}$C NMR (100 MHz, DMSO-$d_6$) $\delta$ 173.94, 139.42, 131.63, 122.93, 119.03, 44.09, 31.29. HRMS calcd for $C_{20}H_{22}N_2O_2$, 322.16813; found, 323.17515 [M + H]$^+$.

**Step 2.** A mixture of amide **23a** (322.4 mg, 1.0 mmol) and $LiAlH_4$ (2.0 mL, 2.0 mmol, 1 N in THF) in THF (40 mL) was refluxed until the disappearance of the amide from the TLC plates. After cooling down to room temperature, the reaction was quenched with the addition of water and aqueous NaOH (15%) as described in the literature[42] and then extracted with diethyl ether (2 × 40 mL). The combined organic phases were washed with brine and dried over $MgSO_4$. Removal of the solvent gave the free amine product which was purified by column chromatography to give **24a** (255.3 mg, 85%) as a pale yellow solid. $R_f$ = 0.48 (4:1, hexane/ethyl acetate). $^1$H NMR (600 MHz, $CDCl_3$) $\delta$ 7.18 (4H, m), 6.69 (2H, tt, $J$ = 7.8 Hz, 0.6 Hz), 6.60 (4H, dd, $J$ = 9.0 Hz, 0.6 Hz), 3.72 (2H, s), 2.99 (4H, d, $J$ = 6.6 Hz), 1.92 (4H, d, $J$ = 6.6 Hz), 1.59 (2H, m), 1.03 (4H, m); $^{13}$C NMR (100 MHz, $CDCl_3$) $\delta$ 148.71, 129.45, 117.19, 112.82, 50.65, 37.94, 30.96. *m*/*z* (EI$^+$) calcd for $C_{20}H_{26}N_2$, 294.5; found, 294.5 M$^+$. Anal. Calcd for $C_{20}H_{26}N_2$: C, 81.59; H, 8.90; N, 9.51. Found: C, 81.45; H, 8.98; N, 9.27.

***N,N′*-Diphenyl-1,4-naphthalenedimethanamine (24b).** The title compound was prepared according to general procedure D as a white solid in 61% yield (2 steps). $R_f$ = 0.51 (4:1, hexane/ethyl acetate). $^1$H NMR (600 MHz, $CDCl_3$) $\delta$ 8.15 (2H, dd, $J$ = 6.0 Hz, 3.0 Hz), 7.58 (2H, dd, $J$ = 6.0 Hz, 3.0 Hz), 7.51 (2H, s), 7.23 (4H, t, $J$ = 7.8 Hz), 6.77 (2H, t, $J$ = 7.2 Hz), 6.71 (4H, d, $J$ = 7.2 Hz), 4.76 (4H, s), 4.12 (2H, br); $^{13}$C NMR (100 MHz, DMSO-$d_6$) $\delta$ 148.24, 134.54, 132.15, 129.56, 126.51, 126.02, 124.58, 117.97, 113.06, 46.75. *m*/*z* (EI$^+$) calcd for $C_{24}H_{22}N_2$, 338.5; found, 338.4 M$^+$. Anal. Calcd for $C_{24}H_{22}N_2$: C, 85.17; H, 6.55; N, 8.31. Found: C, 84.71; H, 6.47; N, 8.11.

***N,N′*-Diphenyl-1,4-benzenediethanamine (24c).** Starting from 1,4-phenylenediacetic acid, general procedure D provided the title compound as a yellow solid in 49% yield (2 steps). $R_f$ = 0.47 (4:1, hexane/ethyl acetate). $^1$H NMR (600 MHz, $CDCl_3$) $\delta$ 7.20 (8H, m), 6.73 (2H, t, $J$ = 7.2 Hz), 6.64 (4H, d, $J$ = 7.2 Hz), 3.69 (2H, br), 3.42 (4H, t, $J$ = 7.2 Hz), 2.92 (4H, t, $J$ = 7.2 Hz); $^{13}$C NMR (100 MHz, $CDCl_3$) $\delta$ 148.21, 137.60, 129.49, 129.22, 117.87, 113.18, 45.24, 35.32. *m*/*z* (EI$^+$) calcd for $C_{22}H_{24}N_2$, 316.5; found, 316.4 M$^+$. Anal. Calcd for $C_{22}H_{24}N_2$: C, 83.50; H, 7.64; N, 8.85. Found: C, 83.63; H, 7.65; N, 8.64.

**2,3,5,6-Tetramethyl-*N,N′*-diphenyl-1,4-benzenedimethanamine (25a).** From 2,3,5,6-tetramethyl-1,4-benzenedicarboxaldehyde (95.1 mg, 0.5 mmol) and aniline (0.11 mL, 1.05 mmol) with $NaBH(OAc)_3$ (317.9 mg, 1.5 mmol) and an activated molecular sieve, the modified general procedure C delivered **25a** (110.9 mg, 64%) as a white solid. $R_f$ = 0.67 (4:1, hexane/ethyl acetate). $^1$H NMR (600 MHz, $CDCl_3$) $\delta$ 7.26 (4H, m), 6.78 (2H, t, $J$ = 7.8

Hz), 6.71 (4H, d, $J$ = 7.8 Hz), 4.31 (4H, s), 3.48 (2H, br), 2.32 (12H, s); $^{13}$C NMR (100 MHz, $CDCl_3$) $\delta$ 148.44, 134.94, 134.31, 129.53, 117.67, 112.73, 43.70, 16.52. $m/z$ ($EI^+$) calcd for $C_{24}H_{31}N_2$, 344.7; found, 344.5 $M^+$. Anal. Calcd for $C_{24}H_{31}N_2$: C, 83.68; H, 8.19; N, 8.13. Found: C, 83.34; H, 8.09; N, 7.89.

***N,N′*-Diphenyl-9,10-anthracenedimethanamine (25b).** The title compound was prepared according to general procedure C as a yellow solid in 98% yield. $R_f$ = 0.54 (4:1, hexane/ethyl acetate). $^1$H NMR (400 MHz, $CDCl_3$) $\delta$ 8.36 (4H, dd, $J$ = 7.2 Hz, 3.2 Hz), 7.55 (4H, dd, $J$ = 7.2 Hz, 3.2 Hz), 7.32 (4H, t, $J$ = 8.0 Hz), 6.85 (6H, m), 5.20 (4H, s), 3.98 (2H, br); $^{13}$C NMR (150 MHz, $CDCl_3$) $\delta$ 148.51, 130.86, 130.53, 129.68, 126.50, 125.13, 118.15, 112.94, 41.34. HRMS calcd for $C_{31}H_{24}N_2$, 388.19395; found, 389.20095 $[M + H]^+$. Anal. Calcd for $C_{31}H_{24}N_2$: C, 86.56; H, 6.23; N, 7.21. Found: C, 86.35; H, 6.13; N, 6.82.

***N,N′*-Diphenyl-1,3-benzenedimethanamine (25c).**[54] From *m*-phthalaldehyde (536.0 mg, 4.0 mmol), aniline (0.77 mL, 2.1 mmol), and $NaBH(OAc)_3$ (2.54 g, 12.0 mmol), general procedure C delivered **22c** (1.02 g, 88%) as a pale yellow solid. $R_f$= 0.57 (4:1, hexane/ethyl acetate). $^1$H NMR (400 MHz, $CDCl_3$) $\delta$ 7.43 (1H, s), 7.36 (3H, m), 7.23 (4H, m), 6.78 (2H, t, $J$ = 7.8 Hz), 6.68 (4H, d, $J$ = 7.8 Hz), 4.36 (4H, s), 4.07 (2H, s); $^{13}$C NMR (100 MHz, $CDCl_3$) $\delta$ 148.26, 140.09, 129.44, 129.03, 126.74, 126.54, 117.77, 113.05, 48.42. $m/z$ ($EI^+$) calcd for $C_{20}H_{20}N_2$, 318.5; found, 318.4. Anal. Calcd for $C_{20}H_{20}N_2$: C, 83.30; H, 6.99; N, 9.71. Found: C, 83.31; H, 6.95; N, 9.70.

**2,5-Dimethyl-*N,N′*-diphenyl-1,4-benzenedimethanamine (26a).**[55] 2,5-Bis(chloromethyl)-*p*-xylene (406.2 mg, 2.0 mmol) and aniline (0.38 mL, 4.2 mmol) in absolute ethanol (15 mL) with pyridine (0.81 mL, 10 mmol) were heated to reflux overnight. The solvent was removed to minimum volume, followed by addition of ethyl acetate (15 mL). The resulting mixture was washed with brine and dried over $MgSO_4$. Removal of the solvent gave the crude product which was purified by column chromatography to give **26a** (433.5 mg, 68%) as a pale yellow solid. $R_f$ = 0.54 (4:1, hexane/ethyl acetate). $^1$H NMR (400 MHz, $CDCl_3$) $\delta$ 7.21 (6H, m), 6.76 (2H, t, $J$ = 7.2 Hz), 6.67 (4H, d, $J$ = 8.0 Hz), 4.24 (4H, s), 3.90 (2H, br), 2.32 (6H, s); $^{13}$C NMR (100 MHz, $CDCl_3$) $\delta$ 148.42, 136.25, 134.21, 130.85, 129.50, 117.82, 113.04, 46.44, 18.68. $m/z$ ($EI^+$) calcd for $C_{22}H_{24}N_2$, 316.5; found, 316.4 $M^+$. Anal. Calcd for $C_{22}H_{24}N_2$: C, 83.50; H, 7.64; N, 8.85. Found: C, 83.46; H, 7.38; N, 9.01.

***N,N′*-Diphenyl-1,2-benzenedimethanamine (26b).** To a solution of aniline (1.8 mL, 20 mmol) and pyridine (1.62 mL, 20 mmol) in absolute ethanol (10 mL) was added dropwise a solution of *o*-xylylene dibromide (527.9 mg, 2.0 mmol) in ethanol (10 mL) at −20 °C. The reaction mixture was stirred at −20 °C for 24 h, at which point the solvent was removed to minimum volume followed by addition of ethyl acetate (15 mL). The resulting mixture was washed with brine and dried over $MgSO_4$. Removal of the solvent gave the crude product which was purified by column chromatography to give **26b** (333.5 mg, 58%) as a white solid. $R_f$ = 0.53 (4:1, hexane/ethyl acetate). $^1$H NMR (600 MHz, $CDCl_3$) $\delta$ 7.44 (2H, m), 7.30 (2H, m), 7.19 (4H, tt, $J$ = 6.6 Hz, 1.8 Hz), 6.77 (2H, t, $J$ = 7.8 Hz), 6.68 (4H, d, $J$ = 7.8 Hz), 4.60 (2H, br), 4.40 (4H, s); $^{13}$C NMR (100 MHz, $CDCl_3$) $\delta$ 148.13, 137.44, 129.56, 129.51, 131.17, 118.21, 113.41, 46.55. HRMS calcd for $C_{20}H_{20}N_2$, 318.16265; found, 319.16957 $[M + H]^+$. Anal. Calcd for $C_{20}H_{20}N_2$: C, 83.30; H, 6.99; N, 9.71. Found: C, 83.32; H, 6.97; N, 9.72.

***N,N′,N″*-Triphenyl-1,3,5-benzenetrimethanamine (29).** Starting from trimesoyl chloride, the modified general procedure D provided the title compound **29** as a pale yellow solid in 80% yield (2 steps). $R_f$ = 0.74 (2:1, hexane/ethyl acetate). $^1$H NMR (400 MHz, $CDCl_3$) $\delta$ 7.31(3H, s); 7.18 (6H, m), 6.74 (3H, tt, $J$ = 7.2 Hz, 0.8 Hz), 6.63 (6H, m), 4.32 (6H, s), 4.03 (3H, s); $^{13}$C NMR (100 MHz, $CDCl_3$) $\delta$148.24, 140.60, 129.44, 125.66, 117.84, 113.10, 48.42. $m/z$ ($EI^+$) calcd for $C_{27}H_{27}N_3$ 393.5; Found 393.5. Ana. Calcd for $C_{27}H_{27}N_3$: C, 82.41; H, 6.92; N, 10.68; Found: C, 81.99; H, 6.86; N, 10.40.

**α,α′-Dimethyl-*N,N′*-diphenyl-1,4-benzenedimethanamine (30a).**[56] Starting from 1,4-diacetylbenzene (648.8 mg, 4.0 mmol), aniline (0.77 mL, 8.4 mmol), and $NaBH(OAc)_3$ (2.54 g, 12.0 mmol) with HOAc (0.46 mL, 8.0 mmol), the modified general procedure C delivered **30a** (238.5 mg, 19%) as a pale white solid. $R_f$ = 0.44 (4:1, hexane/ethyl acetate). $^1$H NMR (400 MHz, $CDCl_3$) $\delta$ 7.32 (4H, s), 7.11 (4H, t, $J$ = 7.8 Hz), 6.66 (2H, m), 6.52 (4H, m), 4.48 (2H, m), 4.01 (2H, s), 1.52 (3H, s), 1.50 (3H, s); $^{13}$C NMR (100 MHz, $CDCl_3$) $\delta$ 147.51, 143.93, 143.96, 129.30, 126.35, 117.36, 117.35, 113.43, 53.31, 53.29, 25.01, 24.91. HRMS calcd for $C_{22}H_{24}N_2$, 316.19395; found, 317.20095 $[M + H]^+$. Anal. Calcd for $C_{22}H_{24}N_2$: C, 83.50; H, 7.64; N, 8.85. Found: C, 83.05; H, 7.72; N, 8.68.

***N,N′*-Dimethyl-*N,N′*-diphenyl-1,4-benzenedimethanamine (30b).** Starting from 1,4-benzenedialdehyde (536.0 mg, 4.0 mmol), *N*-methyl-benzenenamine (0.91 mL, 8.4 mmol), and $NaBH(OAc)_3$ (2.54 g, 12.0 mmol), general procedure C delivered the title compound **30b** (1.18 g, 93%) as a pale white solid. $R_f$ = 0.69 (4:1, hexane/ethyl acetate). $^1$H NMR (400 MHz, $CDCl_3$) $\delta$ 7.24 (4H, m), 7.19 (4H, s), 6.75 (6H, m), 4.53 (4H, s), 3.02 (6H, s); $^{13}$C NMR (100 MHz, $CDCl_3$) $\delta$ 149.90, 137.83, 129.35, 127.16, 116.69, 112.52, 56.53, 38.69. HRMS calcd for $C_{22}H_{24}N_2$, 316.19395; found, 317.20085 $[M + H]^+$. Anal. Calcd for $C_{22}H_{24}N_2$: C, 83.50; H, 7.64; N, 8.85. Found: C, 83.36; H, 7.63; N, 8.87.

***N,N′*-Bis[2-(phenylamino)ethyl]-1,4-benzenedimethanamine (30c).** The title compound was prepared according to general procedure C as a pale white solid in 56% yield. $R_f$ = 0.66 (3:1, $CH_2Cl_2$/MeOH). $^1$H NMR (600 MHz, $CDCl_3$) $\delta$ 7.29 (4H, s), 7.18 (4H, t, $J$ = 5.2 Hz), 6.71 (2H, t, $J$ = 4.8 Hz), 6.64 (4H, d, $J$ = 6 Hz), 4.12 (2H, br), 3.81 (4H, s), 3.23 (4H, t, $J$ = 3.6 Hz), 2.91 (4H, t, $J$ = 3.6 Hz); $^{13}$C NMR (100 MHz, $CDCl_3$) $\delta$ 148.64, 139.18, 129.38, 131.36, 117.53, 113.13, 53.49, 48.17, 43.65. mp 42−43 °C. HRMS calcd for $C_{24}H_{30}N_4$, 374.24705; found, 375.25391 $[M + H]^+$. A salt form of **30c** was prepared as a white solid for the elemental analysis. Anal. Calcd for $C_{24}H_{30}N_4$·2HCl: C, 64.42; H, 7.21; N, 12.52. Found: C, 64.32; H, 7.21; N, 12.30.

***N,N′*-Bis(phenylmethyl)-1,4-benzenedimethanamine (30d).**[57] Starting from 1,4-benzenedialdehyde (536.0 mg, 4.0 mmol), benzenemethanamine (0.92 mL, 8.4 mmol), and $NaBH(OAc)_3$ (2.54 g, 12.0 mmol), general procedure C delivered the title compound **30d** (852.8 mg, 67%) as a pale yellow solid. $R_f$ = 0.69 (ethyl acetate with 2% $NH_4OH$). $^1$H NMR (600 MHz, DMSO-$d_6$) $\delta$ 7.32 (8H, m), 7.31 (4H, s), 7.22 (2H, tt, $J$ = 7.2 Hz, 1.2 Hz), 3.66 (4H, s), 3.65 (4H, s), 2.53 (2H, s); $^{13}$C NMR (100 MHz, DMSO-$d_6$) $\delta$ 140.44, 139.12, 131.49, 131.33, 131.26, 127.04, 53.24, 53.00. HRMS calcd for $C_{22}H_{24}N_2$, 316.19395; found. 317.20083 $[M + H]^+$. Anal. Calcd for $C_{22}H_{24}N_2$: C, 83.50; H, 7.64; N, 8.85. Found: C, 83.49; H, 7.72; N, 8.80.

***N,N′*-Bis(4-cyanylphenyl)-1,4-benzenedimethanamine (31a).** The title compound was prepared according to general procedure C as a pale white solid in 57% yield. $R_f$ = 0.25 (1:1, hexane/ethyl acetate). $^1$H NMR (400 MHz, DMSO-$d_6$) $\delta$ 7.42 (4H, d, $J$ = 9.2 Hz), 7.29 (4H, s), 7.26 (2H, t, $J$ = 6.0 Hz), 6.63 (4H, d, $J$ = 9.2 Hz), 4.30 (4H, d, $J$ = 6.0 Hz); $^{13}$C NMR (100 MHz, DMSO-$d_6$) $\delta$ 152.04, 137.68, 133.31, 127.31, 120.54, 112.22, 95.88, 45.41. $m/z$ ($EI^+$) calcd for $C_{22}H_{18}N_4$, 338.4; found, 338.5 $M^+$. Anal. Calcd for $C_{22}H_{18}N_4$: C, 78.08; H, 5.36; N, 16.56. Found: C, 77.84; H, 5.38; N, 16.17.

***N,N′*-Bis(4-nitrophenyl)-1,4-benzenedimethanamine (31b).** The title compound was prepared according to general procedure C as a yellow solid in 62% yield. $R_f$ = 0.24 (1:1, hexane/ethyl acetate). $^1$H NMR (400 MHz, DMSO-$d_6$) $\delta$ 7.97 (4H, d, $J$ = 9.2 Hz), 7.88 (2H, t, $J$ = 5.6 Hz), 7.33 (4H, s), 6.66 (4H, d, $J$ = 9.2 Hz), 4.39 (4H, d, $J$ = 5.6 Hz); $^{13}$C NMR (100 MHz, DMSO-$d_6$) $\delta$ 154.40, 137.42, 135.86, 127.42, 126.14, 45.50. HRMS calcd for $C_{20}H_{18}N_4O_4$, 378.18231; found, 379.13980 $[M + H]^+$. Anal. Calcd for $C_{20}H_{18}N_4O_4$: C, 63.48; H, 4.79; N, 14.81. Found: C, 63.53; H, 4.91; N, 14.76.

***N,N′*-Bis(3-fluorophenyl)-1,4-benzenedimethanamine (31g).** The title compound was prepared according to general procedure C as a white solid in 62% yield. $R_f$ = 0.35 (4:1, hexane/ethyl acetate). $^1$H NMR (400 MHz, $CDCl_3$) $\delta$ 7.35 (4H, s), 7.10 (2H, q, $J$ = 8.4 Hz), 6.44−6.39 (4H, m), 6.32 (2H, dt, $J$ = 11.6 Hz, 2.4

Hz), 4.32 (4H, s), 4.20 (2H, s); $^{13}$C NMR (100 MHz, $CDCl_3$) $\delta$ 164.30 (d, $J = 241.3$ Hz), 149.98 (d, $J = 11.3$ Hz), 138.24, 130.51 (d, $J = 10.6$ Hz), 131.01, 108.94 (d, $J = 2.3$ Hz), 104.22 (d, $J = 21.2$ Hz), 99.74 (d, $J = 25.0$ Hz), 48.06. HRMS calcd for $C_{20}H_{18}N_2F_2$, 324.14380; found, 325.15076 $[M + H]^+$. Anal. Calcd for $C_{20}H_{18}N_2F_2$: C, 74.06; H, 5.59; N, 8.64. Found: C, 73.96; H, 5.60; N, 8.56.

***N,N′*-Bis(3-nitrophenyl)-1,4-benzenedimethanamine (31h).** The title compound was prepared according to general procedure C as a yellow solid in 55% yield. $R_f = 0.52$ (1:1, hexane/ethyl acetate). $^1$H NMR (400 MHz, DMSO-$d_6$) $\delta$ 7.34−7.26 (10H, m), 7.00−6.95 (4H, m), 4.32 (4H, d, $J = 6.0$ Hz); $^{13}$C NMR (100 MHz, DMSO-$d_6$) $\delta$ 149.65, 148.76, 137.78, 129.95, 127.36, 118.45, 109.95, 105.57, 45.91. HRMS calcd for $C_{20}H_{18}N_4O_4$, 378.18231; found, 379.13964 $[M + H]^+$. Anal. calcd for $C_{20}H_{18}N_4O_4$: C, 63.48; H, 4.79; N, 14.81. Found: C, 63.46; H, 4.83; N, 14.77.

***N,N′*-Bis(3-methoxyphenyl)-1,4-benzenedimethanamine (31i).** The title compound was prepared according to general procedure C as a white solid in 94% yield. $R_f = 0.48$ (2:1, hexane/ethyl acetate). $^1$H NMR (400 MHz, $CDCl_3$) $\delta$ 7.35 (4H, s), 7.09 (2H, d, $J = 8.0$ Hz), 6.32−6.26 (4H, m), 6.20 (2H, d, $J = 2.4$ Hz), 4.32 (4H, s), 4.12 (2H, br), 3.76 (6H, s); $^{13}$C NMR (100 MHz, $CDCl_3$) $\delta$ 160.99, 149.66, 138.55, 130.19, 127.99, 106.19, 102.84, 99.07, 55.25, 48.19. HRMS calcd for $C_{22}H_{24}N_2O_2$, 348.18378; found, 349.19073 $[M + H]^+$. Anal. Calcd for $C_{22}H_{24}N_2O_2$: C, 75.83; H, 6.94; N, 8.04. Found: C, 75.79; H, 6.93; N, 8.02.

***N,N′*-Bis(2-fluorophenyl)-1,4-benzenedimethanamine (31k).** The title compound was prepared according to general procedure C as a white solid in 44% yield. $R_f = 0.58$ (4:1, hexane/ethyl acetate). $^1$H NMR (600 MHz, $CDCl_3$) $\delta$ 7.38 (4H, s), 7.02−6.97 (4H, m), 6.71−6.64 (4H, m), 4.45 (2H, br), 4.38 (4H, s); $^{13}$C NMR (100 MHz, $CDCl_3$) $\delta$ 151.75 (d, $J = 236.7$ Hz), 138.26, 136.59 (d, $J = 11.4$ Hz), 127.96, 124.79 (d, $J = 3.1$ Hz), 117.16 (d, $J = 6.8$ Hz), 114.62 (d, $J = 18.2$ Hz), 112.58, 47.79. HRMS calcd for $C_{20}H_{18}N_2F_2$, 324.14380; found, 325.15075 $[M + H]^+$. Anal. Calcd for $C_{20}H_{18}N_2F_2$: C, 74.06; H, 5.59; N, 8.64. Found: C, 74.06; H, 5.62; N, 8.54.

***N,N′*-Bis(2-methoxyphenyl)-1,4-benzenedimethanamine (31l).** The title compound was prepared according to general procedure C as a white solid in 59% yield. $R_f = 0.66$ (2:1, hexane/ethyl acetate). $^1$H NMR (400 MHz, $CDCl_3$) $\delta$ 7.37 (4H, s), 6.87−6.79 (4H, m), 6.70 (2H, td, $J = 8.0$ Hz, 1.2 Hz), 6.62 (2H, dd, $J = 8.0$ Hz, 1.6 Hz), 4.70 (2H, br), 4.35 (4H, s), 3.86 (6H, s); $^{13}$C NMR (100 MHz, $CDCl_3$) $\delta$ 146.97, 138.66, 138.31, 127.97, 121.45, 116.83, 110.24, 109.56, 55.58, 47.95. HRMS calcd for $C_{22}H_{24}N_2O_2$, 348.18378; found, 349.19059 $[M + H]^+$. Anal. Calcd for $C_{22}H_{24}N_2O_2$: C, 75.83; H, 6.94; N, 8.04. Found: C, 75.77; H, 6.96; N, 7.97.

***N,N′*-Di-2-pyridinyl-1,4-benzenedimethanamine 32.** A mixture of 1,4-benzenedialdehyde (2.68 g, 20.0 mmol), 2-aminopyrdine (3.95 g, 42.0 mmol), and $NaBH(OAc)_3$ (12.7 g, 60.0 mmol) in 1,2-dichloroethane (50 mL) was stirred for 5 min, followed by addition of HOAc (2.4 mL, 40.0 mmol). After stirring for 5 h, the reaction was quenched by aqueous NaOH (1.0 N), providing a white precipitate which was collected. The liquid phase was extracted with ethyl acetate (2 × 100 mL). The combined organic phases were washed with brine, dried over anhydrous $MgSO_4$, filtered, and concentrated under reduced pressure to give a solid residue which was combined with the previously collected white solid to give the crude product. The crude product was purified by recrystallization in ethyl acetate to give free base product **32** (3.25 g, 56%) as white crystalline. $^1$H NMR (400 MHz, DMSO-$d_6$) $\delta$ 7.93 (2H, dd, $J = 5.2$ Hz, 0.8 Hz), 7.34 (2H, ddd, $J = 8.4$ Hz, 6.8 Hz, 2.0 Hz), 7.25 (4H, s), 6.96 (2H, t, $J = 6.0$ Hz), 6.45 (4H, m), 4.42 (4H, d, $J = 6.0$ Hz); $^{13}$C NMR (100 MHz, DMSO-$d_6$) $\delta$ 158.66, 147.53, 138.84, 136.60, 127.11, 111.67, 108.11, 43.92. mp 192−194 °C. HRMS Calcd for $C_{18}H_{18}N_4$, 290.15315; found, 291.15997 $[M + H]^+$. Anal. Calcd. for $C_{18}H_{18}N_4$: C, 74.46; H, 6.25; N, 19.30. Found: C, 74.25; H, 6.18; N, 18.98. The analytical data are in agreement with those reported in the literature.[43,44]

**Acknowledgment.** This study was supported in part by a Distinguished Cancer Scientist Development Fund of the Georgia Cancer Coalition, an Emtech Award, a Georgia Research Alliance Award, and NCI R01 CA 109366 (to H.S.). We are grateful to Vladimir Palyulin and Eugene Radchenko (Moscow State University) for helpful discussion and access to the MFTA software.

**Supporting Information Available:** Figures from the competitive binding assay, additional synthetic procedures, and tables of the elemental analyses and the MFTA analysis. This material is available free of charge via the Internet at http://pubs.acs.org.

## References

(1) Palczewski, K.; Kumasaka, T.; Hori, T.; Behnke, C. A.; Motoshima, H.; Fox, B. A.; Le Trong, I.; Teller, D. C.; Okada, T.; Stenkamp, R. E.; Yamamoto, M.; Miyano, M. Crystal structure of rhodopsin: A G protein-coupled receptor. *Science* **2000**, *289*, 739−45.

(2) Rosenkilde, M. M.; Gerlach, L. O.; Jakobsen, J. S.; Skerlj, R. T.; Bridger, G. J.; Schwartz, T. W. Molecular mechanism of AMD3100 antagonism in the CXCR4 receptor: transfer of binding site to the CXCR3 receptor. *J. Biol. Chem.* **2004**, *279*, 3033−41.

(3) Gerlach, L. O.; Skerlj, R. T.; Bridger, G. J.; Schwartz, T. W. Molecular interactions of cyclam and bicyclam non-peptide antagonists with the CXCR4 chemokine receptor. *J. Biol. Chem.* **2001**, *276*, 14153−60.

(4) Tashiro, K.; Tada, H.; Heilker, R.; Shirozu, M.; Nakano, T.; Honjo, T. Signal sequence trap: a cloning strategy for secreted proteins and type I membrane proteins. *Science* **1993**, *261*, 600−3.

(5) Horuk, R. Chemokine receptors. *Cytokine Growth Factor Rev.* **2001**, *12*, 313−35.

(6) Burns, J. M.; Summers, B. C.; Wang, Y.; Melikian, A.; Berahovich, R.; Miao, Z.; Penfold, M. E.; Sunshine, M. J.; Littman, D. R.; Kuo, C. J.; Wei, K.; McMaster, B. E.; Wright, K.; Howard, M. C.; Schall, T. J. A novel chemokine receptor for SDF-1 and I-TAC involved in cell survival, cell adhesion, and tumor development. *J. Exp. Med.* **2006**, *203*, 2201−13.

(7) De Clercq, E. The bicyclam AMD3100 story. *Nat. Rev. Drug Discovery* **2003**, *2*, 581−7.

(8) Fujii, N.; Nakashima, H.; Tamamura, H. The therapeutic potential of CXCR4 antagonists in the treatment of HIV. *Expert Opin. Invest. Drugs* **2003**, *12*, 185−95.

(9) Feng, Y.; Broder, C. C.; Kennedy, P. E.; Berger, E. A. HIV-1 entry cofactor: functional cDNA cloning of a seven-transmembrane, G protein-coupled receptor. *Science* **1996**, *272*, 872−7.

(10) Oberlin, E.; Amara, A.; Bachelerie, F.; Bessia, C.; Virelizier, J. L.; Arenzana-Seisdedos, F.; Schwartz, O.; Heard, J. M.; Clark-Lewis, I.; Legler, D. F.; Loetscher, M.; Baggiolini, M.; Moser, B. The CXC chemokine SDF-1 is the ligand for LESTR/fusin and prevents infection by T-cell-line-adapted HIV-1. *Nature* **1996**, *382*, 833−5.

(11) Tachibana, K.; Hirota, S.; Iizasa, H.; Yoshida, H.; Kawabata, K.; Kataoka, Y.; Kitamura, Y.; Matsushima, K.; Yoshida, N.; Nishikawa, S.; Kishimoto, T.; Nagasawa, T. The chemokine receptor CXCR4 is essential for vascularization of the gastrointestinal tract. *Nature* **1998**, *393*, 591−4.

(12) Muller, A.; Homey, B.; Soto, H.; Ge, N.; Catron, D.; Buchanan, M. E.; McClanahan, T.; Murphy, E.; Yuan, W.; Wagner, S. N.; Barrera, J. L.; Mohar, A.; Verastegui, E.; Zlotnik, A. Involvement of chemokine receptors in breast cancer metastasis. *Nature* **2001**, *410*, 50−6.

(13) Liang, Z.; Wu, T.; Lou, H.; Yu, X.; Taichman, R. S.; Lau, S. K.; Nie, S.; Umbreit, J.; Shim, H. Inhibition of breast cancer metastasis by selective synthetic polypeptide against CXCR4. *Cancer Res.* **2004**, *64*, 4302−8.

(14) Kucia, M.; Jankowski, K.; Reca, R.; Wysoczynski, M.; Bandura, L.; Allendorf, D. J.; Zhang, J.; Ratajczak, J.; Ratajczak, M. Z. CXCR4-SDF-1 signalling, locomotion, chemotaxis and adhesion. *J. Mol. Histol.* **2004**, *35*, 233−45.

(15) Trent, J. O.; Wang, Z. X.; Murray, J. L.; Shao, W.; Tamamura, H.; Fujii, N.; Peiper, S. C. Lipid bilayer simulations of CXCR4 with inverse agonists and weak partial agonists. *J. Biol. Chem.* **2003**, *278*, 47136−44.

(16) Ueda, S.; Oishi, S.; Wang, Z. X.; Araki, T.; Tamamura, H.; Cluzeau, J.; Ohno, H.; Kusano, S.; Nakashima, H.; Trent, J. O.; Peiper, S. C.; Fujii, N. Structure-activity relationships of cyclic peptide-based chemokine receptor CXCR4 antagonists: disclosing the importance of side-chain and backbone functionalities. *J. Med. Chem.* **2007**, *50*, 192−8.

(17) Tamamura, H.; Tsutsumi, H.; Masuno, H.; Mizokami, S.; Hiramatsu, K.; Wang, Z.; Trent, J. O.; Nakashima, H.; Yamamoto, N.; Peiper, S. C.; Fujii, N. Development of a linear type of low molecular weight CXCR4 antagonists based on T140 analogs. *Org. Biomol. Chem.* **2006**, *4*, 2354−7.

(18) Tamamura, H.; Ojida, A.; Ogawa, T.; Tsutsumi, H.; Masuno, H.; Nakashima, H.; Yamamoto, N.; Hamachi, I.; Fujii, N. Identification of a new class of low molecular weight antagonists against the chemokine receptor CXCR4 having the dipicolylamine-zinc(II) complex structure. *J. Med. Chem.* **2006**, *49*, 3412−5.

(19) Tamamura, H.; Hiramatsu, K.; Ueda, S.; Wang, Z.; Kusano, S.; Terakubo, S.; Trent, J. O.; Peiper, S. C.; Yamamoto, N.; Nakashima, H.; Otaka, A.; Fujii, N. Stereoselective synthesis of [L-Arg-L/D-3-(2-naphthyl)alanine]-type (*E*)-alkene dipeptide isosteres and its application to the synthesis and biological evaluation of pseudopeptide analogues of the CXCR4 antagonist FC131. *J. Med. Chem.* **2005**, *48*, 380−91.

(20) Hatse, S.; Princen, K.; Gerlach, L. O.; Bridger, G.; Henson, G.; De Clercq, E.; Schwartz, T. W.; Schols, D. Mutation of Asp(171) and Asp(262) of the chemokine receptor CXCR4 impairs its coreceptor function for human immunodeficiency virus-1 entry and abrogates the antagonistic activity of AMD3100. *Mol. Pharmacol.* **2001**, *60*, 164−73.

(21) Schwarz, M. K.; Wells, T. N. New therapeutics that modulate chemokine networks. *Nat. Rev. Drug Discovery* **2002**, *1*, 347−58.

(22) Scozzafava, A.; Mastrolorenzo, A.; Supuran, C. T. Non-peptidic chemokine receptors antagonists as emerging anti-HIV agents. *J. Enzyme Inhib. Med. Chem.* **2002**, *17*, 69−76.

(23) Hendrix, C. W.; Flexner, C.; MacFarland, R. T.; Giandomenico, C.; Fuchs, E. J.; Redpath, E.; Bridger, G.; Henson, G. W. Pharmacokinetics and safety of AMD-3100, a novel antagonist of the CXCR-4 chemokine receptor, in human volunteers. *Antimicrob. Agents Chemother.* **2000**, *44*, 1667−73.

(24) Princen, K.; Schols, D. HIV chemokine receptor inhibitors as novel anti-HIV drugs. *Cytokine Growth Factor Rev.* **2005**, *16*, 659−77.

(25) De Clercq, E. HIV-chemotherapy and -prophylaxis: new drugs, leads and approaches. *Int. J. Biochem. Cell Biol.* **2004**, *36*, 1800−22.

(26) Several of the analogues described in this paper have been synthesized previously; however, none of them have been reported as potential CXCR4 antagonists.

(27) Liang, X.; Parkinson, J. A.; Weishaupl, M.; Gould, R. O.; Paisey, S. J.; Park, H. S.; Hunter, T. M.; Blindauer, C. A.; Parsons, S.; Sadler, P. J. Structure and dynamics of metallomacrocycles: recognition of zinc xylyl-bicyclam by an HIV coreceptor. *J. Am. Chem. Soc.* **2002**, *124*, 9105−12.

(28) Seely, D. M.; Wu, P.; Mills, E. J. EDTA chelation therapy for cardiovascular disease: a systematic review. *BMC Cardiovasc. Disord.* **2005**, *5*, 32.

(29) Selig, R. A.; White, L.; Gramacho, C.; Sterling-Levis, K.; Fraser, I. W.; Naidoo, D. Failure of iron chelators to reduce tumor growth in human neuroblastoma xenografts. *Cancer Res.* **1998**, *58*, 473−8.

(30) Grier, M. T.; Meyers, D. G. So much writing, so little science: a review of 37 years of literature on edetate sodium chelation therapy. *Ann. Pharmacother.* **1993**, *27*, 1504−9.

(31) Gerlach, L. O.; Jakobsen, J. S.; Jensen, K. P.; Rosenkilde, M. R.; Skerlj, R. T.; Ryde, U.; Bridger, G. J.; Schwartz, T. W. Metal ion enhanced binding of AMD3100 to Asp262 in the CXCR4 receptor. *Biochemistry* **2003**, *42*, 710−7.

(32) The basement membrane Matrigel is an extract of the Englebreth−Holm−Swarm mouse sarcoma. Its major component is laminin, followed by collagen IV, heparan sulfate proteoglycans, entactin, and nidogen. For more information, see the following. Kleinman, H. K.; McGarvey, M. L.; Liotta, L. A.; Robey, P. G.; Tryggvason, K.; Martin, G. R. Isolation and characterization of type IV procollagen, laminin, and heparan sulfate proteoglycan from the EHS sarcoma. *Biochemistry* **1982**, *21*, 6188−93. McGuire, P. G.; Seeds, N. W. The interaction of plasminogen activator with a reconstituted basement membrane matrix and extracellular macromolecules produced by cultured epithelial cells. *J. Cell. Biochem.* **1989**, *40*, 215−7.

(33) Mel'nikov, A. A.; Palyulin, V. A.; Zefirov, N. S. Generation of molecular graphs for QSAR studies. *Dokl. Chem.* **2005**, *402*, 81−5.

(34) Palyulin, V. A.; Radchenko, E. V.; Zefirov, N. S. Molecular field topology analysis method in QSAR studies of organic compounds. *J. Chem. Inf. Comput. Sci.* **2000**, *40*, 659−67.

(35) Tamamura, H.; Hori, A.; Kanzaki, N.; Hiramatsu, K.; Mizumoto, M.; Nakashima, H.; Yamamoto, N.; Otaka, A.; Fujii, N. T140 analogs as CXCR4 antagonists identified as anti-metastatic agents in the treatment of breast cancer. *FEBS Lett.* **2003**, *550*, 79−83.

(36) Mori, T.; Doi, R.; Koizumi, M.; Toyoda, E.; Ito, D.; Kami, K.; Masui, T.; Fujimoto, K.; Tamamura, H.; Hiramatsu, K.; Fujii, N.; Imamura, M. CXCR4 antagonist inhibits stromal cell-derived factor 1-induced migration and invasion of human pancreatic cancer. *Mol. Cancer Ther.* **2004**, *3*, 29−37.

(37) Oonuma, T.; Morimatsu, M.; Nakagawa, T.; Uyama, R.; Sasaki, N.; Nakaichi, M.; Tamamura, H.; Fujii, N.; Hashimoto, S.; Yamamura, H.; Syuto, B. Role of CXCR4 and SDF-1 in mammary tumor metastasis in the cat. *J. Vet. Med. Sci.* **2003**, *65*, 1069−73.

(38) Braun, C. E.; Erit, J. D.; Crooks, G. C. Guanidine structure and hypoglycemia−Some carbocyclic diguanidines. *J. Org. Chem.* **1938**, *3*, 146−52.

(39) Murdock, K. C.; Child, R. G.; Lin, Y.; Warren, J. D.; Fabio, P. F.; Lee, V. J.; Izzo, P. T.; Lang, S. A., Jr.; Angier, R. B.; Citarella, R. V.; Wallace, R. E.; Durr, F. E. Antitumor agents. 2. Bisguanylhydrazones of anthracene-9,10-dicarboxaldehydes. *J. Med. Chem.* **1982**, *25*, 505−18.

(40) Linton, B. R.; Goodman, M. S.; Fan, E.; van Arman, S. A.; Hamilton, A. D. Thermodynamic aspects of dicarboxylate recognition by simple artificial receptors. *J. Org. Chem.* **2001**, *66*, 7313−9.

(41) Abdel-Magid, A. F.; Carson, K. G.; Harris, B. D.; Maryanoff, C. A.; Shah, R. D. Reductive amination of aldehydes and ketones with sodium triacetoxyborohydride. Studies on direct and indirect reductive amination procedures. *J. Org. Chem.* **1996**, *61*, 3849−62.

(42) Micovic, V. M.; Mihailovic, M. L. The reduction of acid amides with lithium aluminum hydride. *J. Org. Chem.* **1953**, *18*, 1190−1200.

(43) Zou, R. Y.; Xu, F. B.; Li, Q. S.; Song, H. B.; Lv, H.; Zhang, Z. Z. 1,4-bis(pyridine-2-aminomethyl)benzene. *Acta Crystallogr., Sect. E: Struct. Rep. Online* **2003**, *59*, O1312−O1313.

(44) Reyes, M. J.; Delgado, F.; Izquierdo, M. L.; Alvarez-Builla, J. Pyridinium *N*-(2′-azinyl)aminides: regioselective synthesis of *N*-(2-pyridyl) substituted polyamines. *Tetrahedron* **2002**, *58*, 8573−9.

(45) Hatse, S.; Princen, K.; Bridger, G.; De Clercq, E.; Schols, D. Chemokine receptor inhibition by AMD3100 is strictly confined to CXCR4. *FEBS Lett.* **2002**, *527*, 255−62.

(46) Cooper, D. M.; Mons, N.; Karpen, J. W. Adenylyl cyclases and the interaction between calcium and cAMP signalling. *Nature* **1995**, *374*, 421−4.

(47) Taussig, R.; Gilman, A. G. Mammalian membrane-bound adenylyl cyclases. *J. Biol. Chem.* **1995**, *270*, 1−4.

(48) Bohm, H. J.; Banner, D.; Bendels, S.; Kansy, M.; Kuhn, B.; Muller, K.; Obst-Sander, U.; Stahl, M. Fluorine in medicinal chemistry. *ChemBioChem* **2004**, *5*, 637−43.

(49) Maienfisch, P.; Hall, R. G. The importance of fluorine in the life science industry. *Chimia* **2004**, *58*, 93−9.

(50) Dolbier, W. R. Fluorine - A powerful tool for enhancement of bioactive compounds. Recent advances in the development of CF3 and SF3 fluorinated building blocks. *Chim. Oggi* **2003**, *21*, 66−9.

(51) David, P.; Mayan, H.; Cohen, H.; Tal, D. M.; Karlish, S. J. D. Guanidinium derivatives act as high-affinity antagonists of Na+ ions in occlusion sites of Na+,K+-ATPase. *J. Biol. Chem.* **1992**, *267*, 1141−9.

(52) Khownium, K.; Wood, S. J.; Miller, K. A.; Balakrishna, R.; Nguyen, T. B.; Kimbrell, M. R.; Georg, G. I.; David, S. A. Novel endotoxin-sequestering compounds with terephthalaldehyde-bis-guanylhydrazone scaffolds. *Bioorg. Med. Chem. Lett.* **2006**, *16*, 1305−8.

(53) Lowe, J. L.; Peak, D. A.; Watkins, T. I. Antituberculous compounds. 8. Phenolic 2-diethylaminoethyl ethers and analogues. *J. Chem. Soc.* **1951**, 3286−92.

(54) Kawaji, T.; Hayashi, K.; Hashimoto, I.; Matsumoto, T.; Thiemann, T.; Mataka, S. Synthesis of 1,2,9,10-tetrakis(*N*-phenylamino) [2.2]-metacyclophane by SMI2-mediated reductive coupling of diimine. *Tetrahedron Lett.* **2005**, *46*, 5277−9.

(55) Nordlander, J. E.; Catalane, D. B.; Eberlein, T. H.; Farkas, L. V.; Howe, R. S.; Stevens, R. M.; Tripoulas, N. A.; Stansfield, R. E.; Cox, J. L.; Payne, M. J.; Viehbeck, A. Preparation of secondary-amines through efficient alkylation of *N*-substituted trifluoroacetamides. *Tetrahedron Lett.* **1978**, 4987−90.

(56) Lai, R. Y.; Surekha, K.; Hayashi, A.; Ozawa, F.; Liu, Y. H.; Peng, S. M.; Liu, S. T. Intra- and intermolecular hydroamination of alkynes catalyzed by ortho-metalated iridium complexes. *Organometallics* **2007**, *26*, 1062−8.

(57) Ashton, P. R.; Chrystal, E. J. T.; Glink, P. T.; Menzer, S.; Schiavo, C.; Stoddart, J. F.; Tasker, P. A.; Williams, D. J. Doubly encircled and double-stranded pseudorotaxanes. *Angew. Chem., Int. Ed. Engl.* **1995**, *34*, 1869−71.

JM070679I